Electromagnetic interference shielding of polypyrrole nanostructures

Robert Moučka [a], Michal Sedlačík [a,*], Jan Prokeš [b], Hayk Kasparyan [c], Stanislav Valtera [c], Dušan Kopecký [c,*],

[a] *Centre of Polymer Systems, Tomas Bata University in Zlín, 760 01 Zlín, Czech Republic, email: msedlacik@utb.cz*

[b] *Faculty of Mathematics and Physics, Charles University, 180 00 Prague 8, Czech Republic, email: jprokes@semi.mff.cuni.cz*

[c] *Faculty of Chemical Engineering, University of Chemistry and Technology, Prague, 166 28 Prague 6, Czech Republic, email: kopeckyd@vscht.cz*

[*] *corresponding authors: kopeckyd@vscht.cz, msedlacik@utb.cz*

Abstract

Polypyrrole (PPy) is an electrically conductive organic material perspective for application in the field of electromagnetic interference shielding (EMI). The presented fundamental study focuses on the shielding efficiency of three various morphologies of PPy (globules, nanotubes and microbarrels). Powdered samples in both protonated and deprotonated form were embedded at various concentrations (1, 3 and 5 % w/w) in a composite system with a transparent silicone matrix cured at temperatures 25 and 150 °C. The ability of PPy to reflect or absorb electromagnetic radiation in the C-band region covering the range from 5.85 to 8.2 GHz was evaluated. The relationship between the morphology of PPy, its DC and AC electrical conductivity, permittivity and shielding efficiency was studied. The PPy nanotubes with the DC conductivity of 60.8 S cm^{-1} exhibited shielding efficiency S_{21} = –13.27 dB at 5 % w/w concentration in the composite, which corresponds to transparency of 21.7 % only. It was found that the magnitude of electrical conductivity together with the aspect ratio of PPy morphology determines the shielding efficiency whereas the type of morphology is responsible for absorption or reflection mechanism of EMI shielding. Hence, the appropriate adjustment of both the electrical conductivity and the morphology should be used in the future lightweight and flexible EMI shields with tunable shielding efficiency and mechanism of shielding.

Keywords: polypyrrole nanostructures; polypyrrole nanotubes; globular polypyrrole; polypyrrole microbarrels; electromagnetic interference shielding; electrical conductivity; deprotonation

1. Introduction

Polypyrrole (PPy) is a representative of conducting polymers, whose electrical properties resemble inorganic semiconductors while it retains mechanical flexibility of organic polymers. The PPy in a basic globular morphology (PPy-G) was studied thoroughly in the past and thus most of its fundamental properties are well known. [1] Nowadays, PPy research is therefore focused on morphologies containing novel nano- and micro- structures. [2]

One of the most intensively studied morphology of PPy are nanotubes (PPy-NT), which have tens to hundreds of nm in diameter and are several μm long. The PPy-NT exhibits higher electrical conductivity (order of tens to hundreds of S cm^{-1}), better long-term stability (from months to years until conductivity deteriorates to half of its initial value) and resistance against deprotonation compared to PPy-G. [3] These extraordinary features of PPy-NT encourage applications in chemistry (catalysis and absorption of chemicals) [4] and electronics (various physical, chemical or bio- sensors, actuators, batteries and supercapacitors). [5]

Our past research in the field of conducting polymers was focused on the development and optimization of PPy morphology including a new kind of uniform structures, such as PPy microbarrels (PPy-MB). [6, 7] We also experimented with switching and tuning of the magnitude of PPy-G and PPy-NT electrical conductivity using protonation and deprotonation approaches by acids and bases, respectively. [8, 9] Moreover, we performed a study whose aim was to find relationships between PPy morphology and long-term stability of its electrical parameters. [10]

Presented work continues in our fundamental research of PPy morphology. Herein, we have focused on electromagnetic interference (EMI) shielding properties (*i.e.* on the PPy ability to attenuate or reflect electromagnetic radiation) of three PPy morphologies (PPy-G, PPy-NT and PPy-MB), each of which was studied in protonated and deprotonated form. The powdered PPy was embedded in a silicone matrix transparent for electromagnetic radiation under the study. As the preparation of samples for EMI shielding measurement plays a key role, we have also tested the contribution of PPy concentration (load) in matrix and temperature of sample preparation. The EMI measurement was made in the C-band region covering frequencies from 5.85 to 8.2 GHz. This region is especially important for the future application of conducting polymers in the radar, wireless and satellite EMI shielding.

Admittedly, PPy have been attracting attention of experts from the field of EMI shielding for several decades. However, most of published results focus on PPy-G and its composites (metallic, carbonaceous, polymeric, etc.) used as a powder in a transparent matrix. Recently, two important reviews written by Jiang et al. [11] and Kumar et al. [12] have been published covering comprehensively this area. It is also worth mentioning various advanced structures based on PPy-G (intermediates

between PPy-G and self-standing supramolecular structures) forming *e.g.* 3D aerogels networks [13] or thin-layered core-shell composites with metallic nanostructures. [14, 15] Those are effective, easy-to-obtain, shielding materials with almost infinite possibilities for modification and tuning. Engineering of supramolecular nano- or micro- structures of PPy is still relatively young and hence experiments devoted to EMI shielding by PPy nano- or micro- structures are rather scarce. From the application point of view, various nano-tubes, wires or fibers which possess high aspect ratio leading to low concentration in their respective composites are very promising. Recently, PPy-NT and PPy fibers have been tested as EMI shielding materials in several experiments. [16-18]

In the light of these works we have tried to focus on the currently most popular nano- and micro-structures of PPy synthesized in the presence of azo-dyes including their deprotonated forms (PPy structures with decreased content of dopants exhibiting similar morphology but low conductivity). Our goal was to obtain fundamental relationship between morphology, DC electrical conductivity of powders, AC conductivity and complex permittivity of their composites in a silicone matrix and shielding properties of PPy in general. According to our best knowledge, such fundamental research in the field of conducting polymers is presented for the first time.

2. Experimental section

2.1 Chemicals

Pyrrole (Sigma-Aldrich, 98%, CAS number 109-97-7), iron(III) chloride hexahydrate (Sigma-Aldrich, 99%, CAS number 10025-77-1), Methyl Orange (Sigma-Aldrich, dye content 85 %, CAS number 547-58-0), Sunset Yellow FCF (Sigma-Aldrich, dye content 90 %, CAS number 2783-94-0), sodium hydroxide (Penta, pure pellets, CAS number 1310-73-2) were used as purchased without any other modification. Distilled water was used as a solvent in all reactions. Sylgard 184/catalyst kit (Dow Corning) was used as a silicone matrix transparent in studied C-band range for PPy dispersion.

2.2 Synthesis of polypyrrole

The PPy-G was synthesized by simple polymerization of pyrrole in aqueous solution of iron(III) chloride hexahydrate. The typical procedure was as follows: 23.38 g (0.086 mol) of iron(III) chloride hexahydrate was dissolved in 600 mL of distilled water and cooled to 5 °C. After temperature stabilization, 6 mL of pyrrole (0.086 mol) were drop-wisely added under vigorous mixing. Thus, molar ratio of monomer to oxidant was 1:1. Black coloured polymer was filtered out after 24 h of polymerization, washed several times with distilled water and ethanol, and finally dried under vacuum at 40 °C. Dried powder was homogenized using a pestle and mortar.

The PPy-NT were synthesized according to a popular soft-template method using Methyl Orange as a support for nanotubular growth. [6] Typically, 2.09 mL of pyrrole (0.03 mol) was dissolved in a 600

mL of 2.5 M solution of Methyl Orange and cooled to 5 °C. After temperature stabilization, 8.12 g of iron(III) chloride hexahydrate (0.03 mol) was dissolved in 69 mL of distilled water and added drop-wisely into the mixed pyrrole solution. Molar ratio of polymer to oxidant was 1:1 in this case as well. The post-processing of PPy-NT after 24 h of polymerization consisted of filtering and Soxhlet extraction by acetone for at least 2 days and subsequent washing by ethanol and distilled water. Obtained powder was also in a vacuum oven at 40 °C and homogenized using a pestle and mortar.

Finally, the PPy-MB was synthesized according to our recently published procedure. [7] Here, 3.12 g of Sunset Yellow FCF dissolved in 690 mL of distilled water created 0.01 M azo-dye solution. 9.31 g of iron(III) chloride hexahydrate (0.034 mol) were dissolved in it. After temperature stabilization at 5 °C, 2.4 mL of pyrrole (0.034 mol) was added under mixing. Even in this last case, molar ratio of monomer to oxidant was 1:1. The remnants of Sunset Yellow FCF were extracted from PPy-MB by Soxhlet extraction for 2 days. Obtained powder was dried in a vacuum oven at 40 °C and homogenized using a pestle and mortar.

2.3 Tuning of polypyrrole DC electrical conductivity

In order to obtain varying but controlled levels of DC electrical conductivity for all prepared PPy morphologies, we followed our recently published deprotonation methods. [9] Briefly, 1 g of above synthesized materials (PPy-G, PPy-NT and PPy-MB) was dissolved in 500 mL of 0.015 M water solution of sodium hydroxide. After 24 h, the polymer was filtered out and washed several times with excess of distilled water, till the filtrate's pH was around 7. The PPy was dried again in the vacuum oven at 40 °C and homogenized with a pestle and mortar.

2.4 Characterization of morphology by electron microscopy

The morphology of all samples was observed by scanning electron microscopy MIRA 3 LMH (Tescan company) under 3 kV of accelerating voltage. All samples were sputter coated by 8 nm of gold to avoid charging and picture deterioration.

2.5 Measurement of DC electrical conductivity

Apparatus for samples with high DC electrical conductivity (> 0.001 S cm^{-1}): room temperature resistivity is measured by four-point method in the van der Pauw arrangement using Keithley 220 Programmable Current Source, Keithley 2010 Multimeter as a voltmeter and Keithley 705 Scanner equipped with Keithley 7052 Matrix Card.

Apparatus for samples with lower DC electrical conductivity (< 0.001 S cm^{-1}): the four-point van der Pauw method in modified configuration consists of Keithley 6220 Programmable Current Source,

Keithley 6485 Picoammeter, Keithley 2000 Multimeter, Keithley 706 Scanner equipped with Keithley 7152l low current Matrix Card, and two Keithley 6517B Electrometers as high impedance voltmeters. Common mode currents are reduced due to the connection and grounding of low impedance terminals. For more details see ref. [10]

2.6 Preparation of samples for EMI shielding measurement

Three sets of samples for EMI shielding containing PPy-G, PPy-NT and PPy-MB, each of them in protonated and deprotonated form, were fabricated by thorough mixing (~5 min) a polydimethylsiloxane (PDMS) elastomer Sylgard 184 with relevant particles concentration (1, 3 or 5 % w/w). Moreover, two samples containing pure azo-dyes involved during the synthesis of PPy-NT (Methyl Orange) and PPy-MB (Sunset Yellow FCF) were prepared to prove no effect of these soft-templates on the final EMI shielding of the samples under investigation. The resulting mixtures were degassed for 15 min under 10 mbar and finally cast into a PTFE mold of 2 mm thickness. The curing was performed at room temperature for 48 h or in an oven pre-heated to 150 °C for 20 min to check whether the elevated temperature during the curing could affect the PPy conductivity resulting in possible decrease of electrical conductivity of composite samples or their EMI shielding. The corresponding test samples for further investigation were cut out to standardized size from the original composite sample sheet.

2.7 Measurement and evaluation of shielding effectiveness

Shielding effectiveness of prepared materials was measured on a PNA-L network analyser (Agilent N5230A) using a C-band (WR 137) waveguide operating within the frequency range of 5.85 to 8.2 GHz. Rectangular samples (35 × 16 mm) matching the inner cross-section of the waveguide were cut out from prepared composite sheets and placed inside of a waveguide section. Measuring the portion of the incident (I_0) electromagnetic wave transmitted through and reflected (I_1) by the sample, scattering parameters S_{21} and S_{11}, respectively, were directly obtained.

$$S_{21}(dB) = 20 \log \frac{I_1}{I_0} \quad (1)$$

$$S_{11}(dB) = 20 \log \frac{I_1}{I_0} \quad (2)$$

While S_{11} gives portion of reflected radiation, S_{21} provides direct information on transmitted radiation through the sample of given thickness; this was constant (t = 2 mm) for all investigated samples.

2.8 Extraction of complex permittivity and AC electrical conductivity

Complex permittivity ($\varepsilon^* = \varepsilon' - j\varepsilon''$) of PPy composites in the silicone matrix was extracted directly from scattering parameters and phase shift measurement according to standard Nicholson-Ross-Weir method. [19, 20]

AC electrical conductivity of PPy composites in the silicone matrix was calculated from frequency dependence of loss part of complex permittivity:

$$\sigma(\omega) = \omega\varepsilon_0\varepsilon'' \tag{3}$$

where ω is angular velocity, ε_0 is permittivity of vacuum, ε'' is the loss part of complex permittivity.

3. Results and discussions

The morphology of all prepared PPy powders is presented in the Figure 1. Both PPy-G and PPy-NT have uniform particles, each with their respective size lying in a relatively narrow range; PPy-G particles are around 1 μm in diameter, while PPy-NT are around 60–80 nm in diameter and several μms long. Uniformity of PPy-MB depicted in the Figure 1c does not reach such level as in the case of PPy-G and PPy-NT. However, the vast majority of PPy-MB are microbarrels with around 3 μm in diameter composed of plates 300 nm thick, some of them with small defects and minor part comprises globular particles of PPy due to the polymerization of pyrrole outside the template. The PPy-NT and PPy-MB exhibit higher aspect ratio compared to PPy-G. The PPy-NT and PPy-MB also inevitably contain small content of azo-dye remnants (up to 1 % w/w), some of them as dopants, some of them as a composite component, which is present in small cavities of particles. [6]

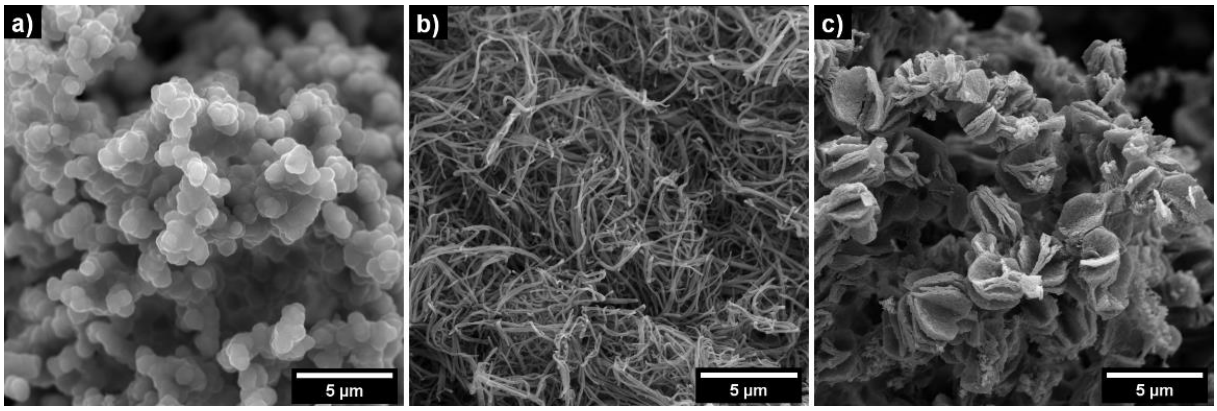

Figure 1 – The morphology of prepared PPy powders: a) globular polypyrrole (PPy-G), b) nanotubular polypyrrole (PPy-NT), c) polypyrrole microbarrels (PPy-MB)

The PPy powders, deprotonated by 0.015 M solution of sodium hydroxide, keep their morphology and hence they are not depicted in a separate figure. An alkali treatment does not have an impact on the shape and size of deprotonated PPy structures; chlorides and azo-dye ions serving as dopants are released during the deprotonation only. [9]

The complete analysis of elemental composition measured by Energy-dispersive X-ray spectroscopy and chemical structure measured by Fourier transform infrared and Raman spectroscopy can be found in our previous works. [6-8]

Morphology and the degree of deprotonation have a strong influence on DC electrical conductivity. Both initial and deprotonated PPy powders were analyzed and DC electrical conductivities of pure azo-dyes Methyl Orange and Sunset Yellow FCF were added to present complex overview of electrical properties of all substances investigated. The results of DC electrical conductivity measurement by the van der Pauw method are presented in the Table 1.

Table 1 – The DC electrical conductivity of PPy and azo-dye powders

Sample	**Initial powder conductivity (S cm^{-1})**	**Deprotonated powder conductivity (S cm^{-1})**
PPy-G	8.9	0.2
PPy-NT	60.8	0.4
PPy-MB	7.2	2.0×10^{-2}
Methyl Orange	$1.3 – 1.4\times10^{-8}$	-
Sunset Yellow FCF	$1.8 – 1.9\times10^{-6}$	-

The most conductive sample is PPy-NT with electrical conductivity of 60.8 S cm^{-1}; on the other side of PPy sample spectrum lies deprotonated PPy-MB with conductivity of only 2.0×10^{-2} S cm^{-1}. All PPy samples have significantly different values of electrical conductivity, which clearly indicates the influence of morphology in the following order: PPy-NT > PPy-G > PPy-MB; and similarly for deprotonated samples. Electrical conductivity of azo-dye Methyl Orange and Sunset Yellow FCF is generally low (1.3×10^{-8} S cm^{-1} and 1.8×10^{-6} S cm^{-1}, respectively), which also means, that the high content of azo-dye in the PPy sample should have a retarding effect on the overall conductivity of the sample. [6]

The EMI shielding properties in the frequency range from 5.85 to 8.2 GHz (WR137) were firstly determined and expressed by S_{21} parameter for Sylgard 184 silicone matrix as well as for low concentration (1 % w/w) of azo-dyes Methyl Orange and Sunset Yellow FCF. According to Figure 2a, Sylgard 184 silicone matrix transparency in given region is around 94.4 %, *i.e.* its shielding efficiency in a composite without PPy is around S_{21} = –0.5 dB, which is negligible. Similarly, the shielding efficiency S_{21} of azo-dyes Methyl Orange (–0.5 dB) and Sunset Yellow FCF (–0.6 dB) in Sylgard 184 corresponds to 93 – 94 % of transparency. The difference between Sylgard 184 transparency and azo-dyes transparency is so small that influence of azo-dye on overall shielding efficiency can be neglected. Moreover, the real presence of remnants of azo-dyes in PPy-NT and PPy-MB is one or two orders lower.

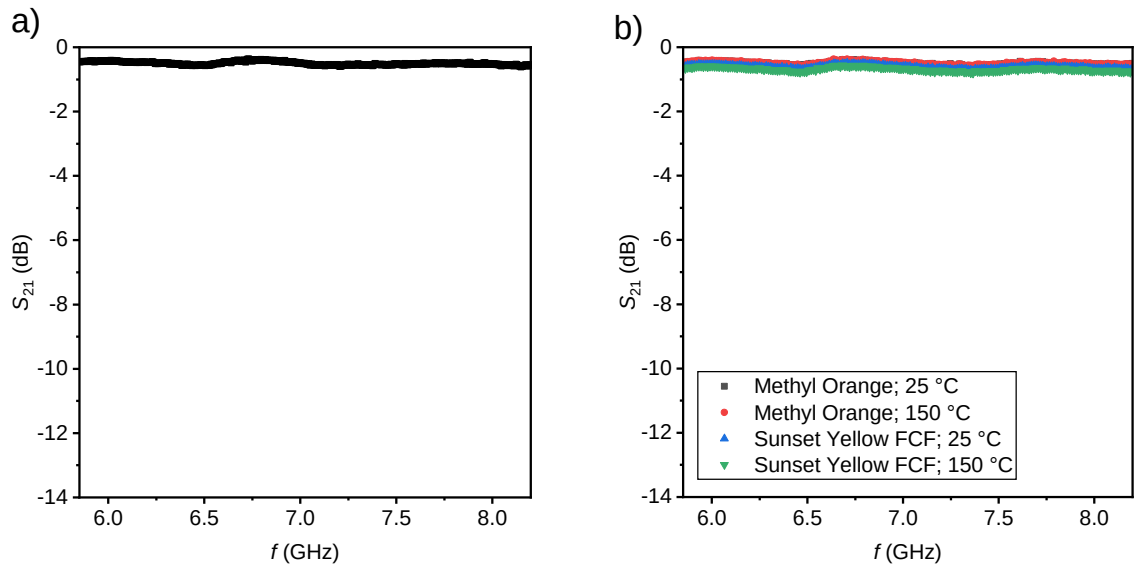

Figure 2 – EMI shielding efficiency expressed by S_{21} parameter of a) Sylgard 184 silicone matrix and b) azo-dyes Methyl Orange and Sunset Yellow FCF with 1 % w/w load in Sylgard 184 matrix cured at 25 °C or 150 °C

The EMI shielding properties of PPy-G, PPy-NT and PPy-MB and their deprotonated counterparts are depicted in the Figure 3. The PPy powders were dispersed at various loads (1, 3 and 5 % w/w) in Sylgard 184 silicone matrix cured at two different temperatures (25 and 150 °C).

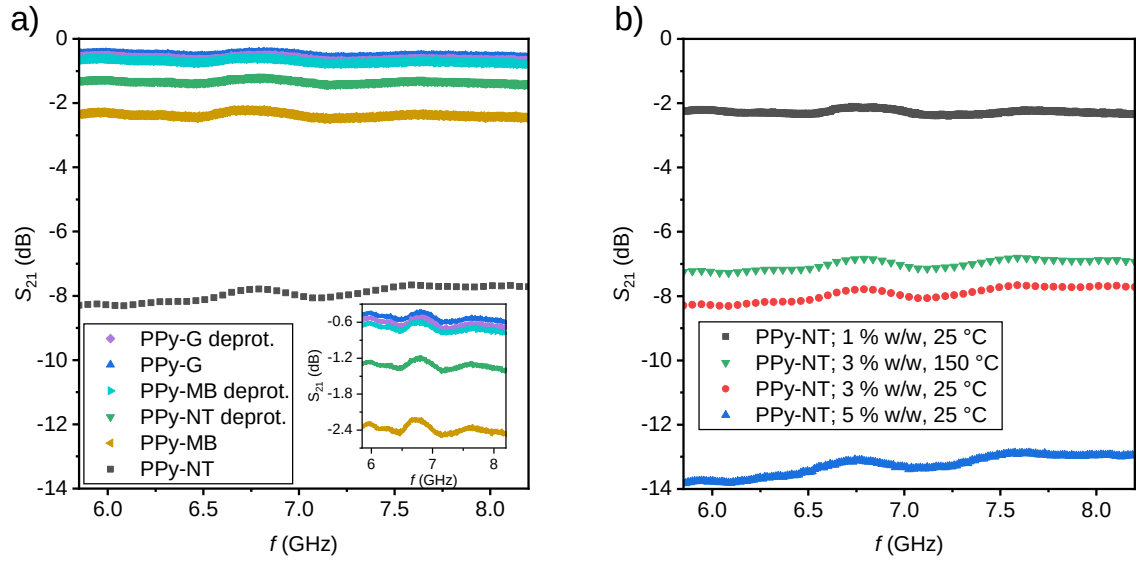

Figure 3 – The EMI shielding properties of a) PPy structures and their deprotonated counterparts (3 % w/w, 25 °C); detailed overview of PPy samples with low shielding efficiency in the inset and b) PPy-NT at various filler loadings and temperatures of sample preparation

The comparison of EMI shielding efficiency expressed by S_{21} parameter in the Figure 3a clearly indicates, that the transparency of PPy structures in the C-band region decreases in order PPy-G (93.3 %) > PPy-MB (76.0 %) > PPy-NT (40.1 %). This trend was found in all samples regardless of load. Moreover, shielding efficiency of all deprotonated samples is lower than their initial counterpart. One of the decisive parameters influencing shielding efficiency is concentration of PPy in the silicone matrix. In the Figure 3b is a comparison of PPy-NT at various concentration (1, 3, 5 % w/w). The highest achieved shielding efficiency S_{21} = –13.27 dB (21.7% of transparency) was obtained for PPy-NT at 5 % w/w prepared at 25 °C. However, it must be noted that observed mechanical stability of the sample at this high PPy concentration is lower. In our previous work [10], we found that electrical properties of PPy structures are highly sensitive to elevated temperatures. The electrical conductivity of PPy-NT with Sylgard 184 composite cured at 150 °C (also in the Figure 3b) decreased, creating difference in shielding efficiency equal to 0.93 dB (4.5 % of transparency). This is the important practical result as PPy is considered as conductive filler in many insulating polymers whose melting point is above 150 °C.

From the scattering parameters and phase shift complex permittivity of all samples was extracted. Figure 4 compares ε' and ε'' of all investigated samples from the viewpoint of morphology while Figure 5 compares the influence of PPy concentration in the silicone matrix on the same parameters.

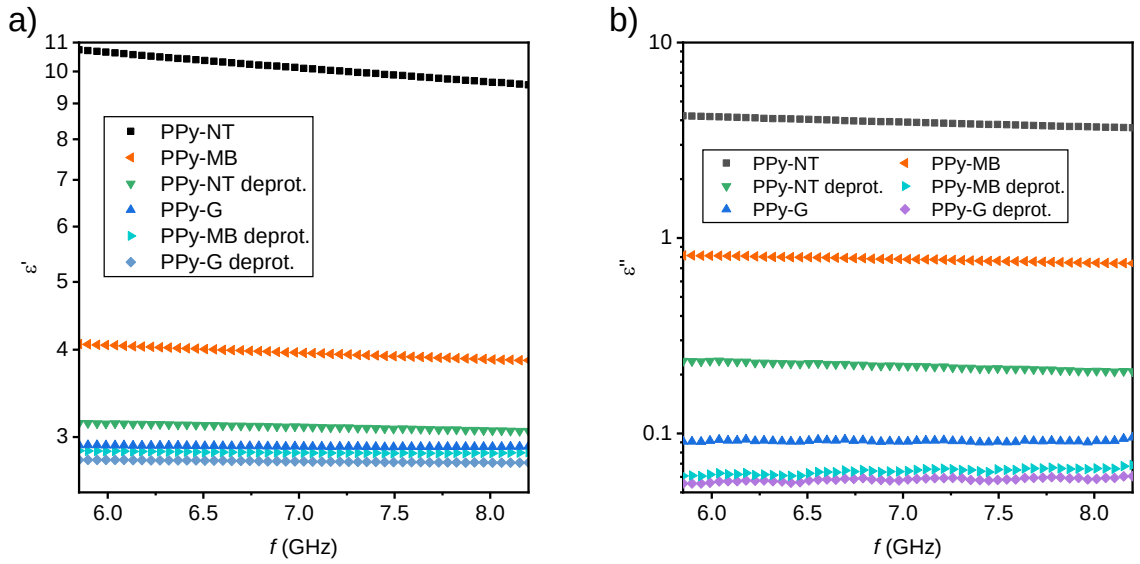

Figure 4 – The a) real and b) imaginary (loss) part of complex permittivity for various PPy morphologies in protonated and deprotonated state (3 % w/w, 25 °C)

Trends in complex permittivity are consistent with the observed trends in scattering parameters and in the case of PPy-NT and PPy-MB the magnitudes are comparable to that of core-shell Ag nanowire@PPy particles and helical nanotubes (at 10 % w/w) recently published by Xie et al. [14, 16]. These results are promising as the preparation of PPy structures via soft-template method is straightforward and exhibits

very high shielding efficiency as confirmed by Hu et al. [18] in their synthesis of PPy in the presence of Indigo Carmine. Figure 5 also emphasizes the influence of PPy concentration on the complex permittivity. It is worth noting that comparable results obtained using non-structured PPy require one order of magnitude higher concentration of PPy in a transparent matrix. [21]

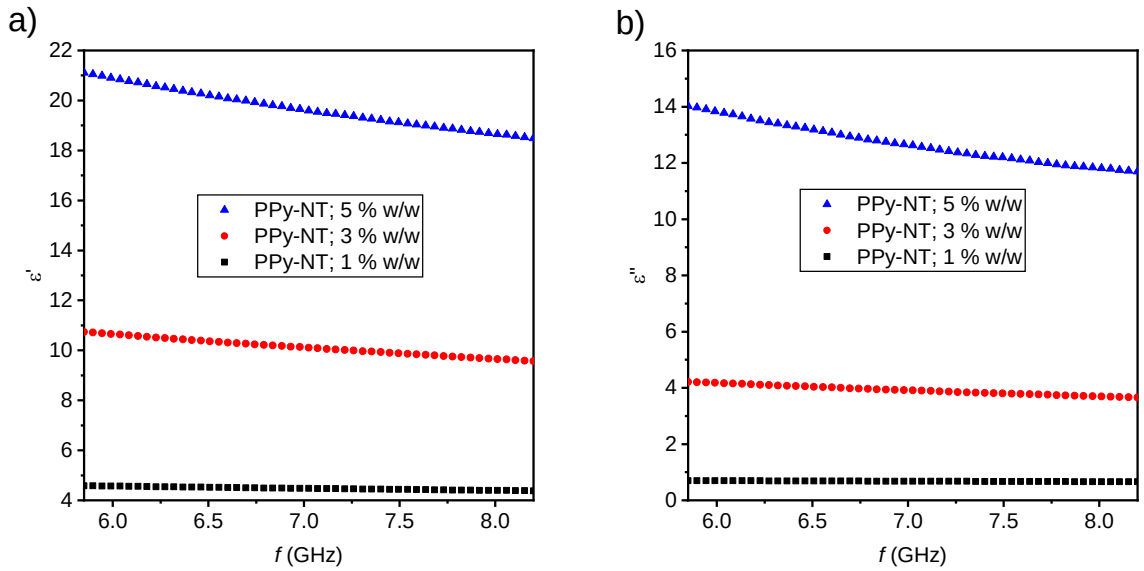

Figure 5 – The a) real and b) imaginary part of complex permittivity of PPy-NT at various concentration in silicone matrix (25 °C)

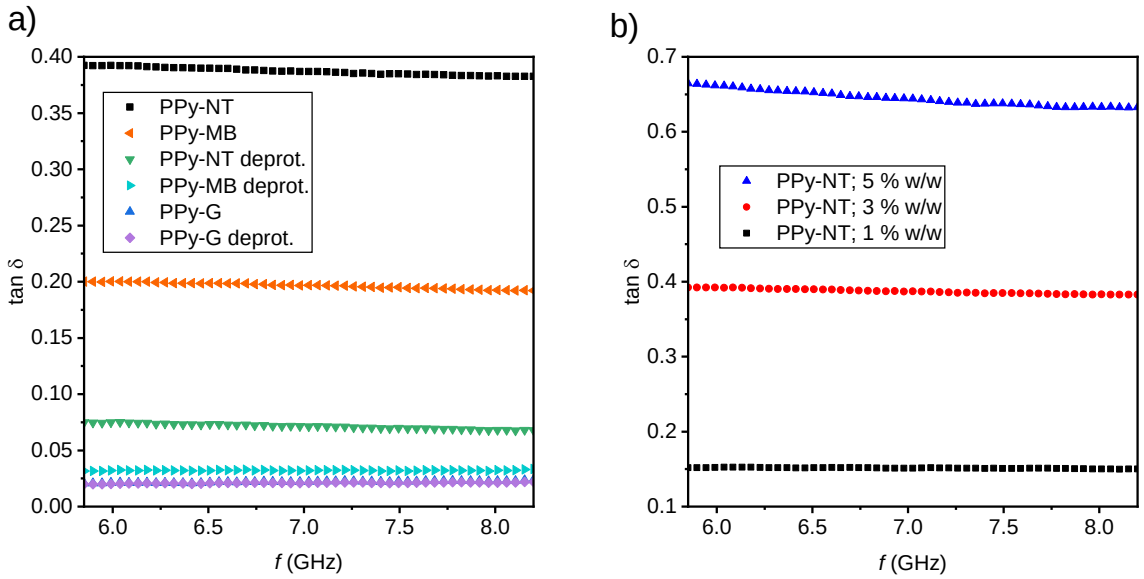

Figure 6 – The dielectric loss tangent of a) various PPy morphologies in protonated and deprotonated state (3 % w/w, 25 °C) and b) PPy-NT at various concentration in the silicone matrix (25 °C)

The calculated dielectric loss tangent (tan $\delta = \varepsilon''/\varepsilon'$) in the Figure 6 provides information about dielectric behavior of all samples. PPy-NT and PPy-MB exhibit generally higher loss for field propagation compared to PPy-G, however, these calculations also point out relatively low AC electrical conductivity (introduced bellow) of all the PPy samples in the silicone matrix.

The depicted shielding efficiency in Figures 3 and complex permittivity in Figure 4 and Figure 5 still does not contain all information about the influence of the morphology of PPy on the shielding efficiency. In order to better distinguish influence of particles' morphology and electrical conductivity, dependence of shielding efficiency of all PPy samples in the silicone matrix vs. DC electrical conductivity of their initial pure powders (Figure 7a) and dependence of AC electrical conductivity of PPy samples in the silicone matrix (for clarity only 3 % w/w, 25 °C) vs. frequency (Figure 7b) were constructed.

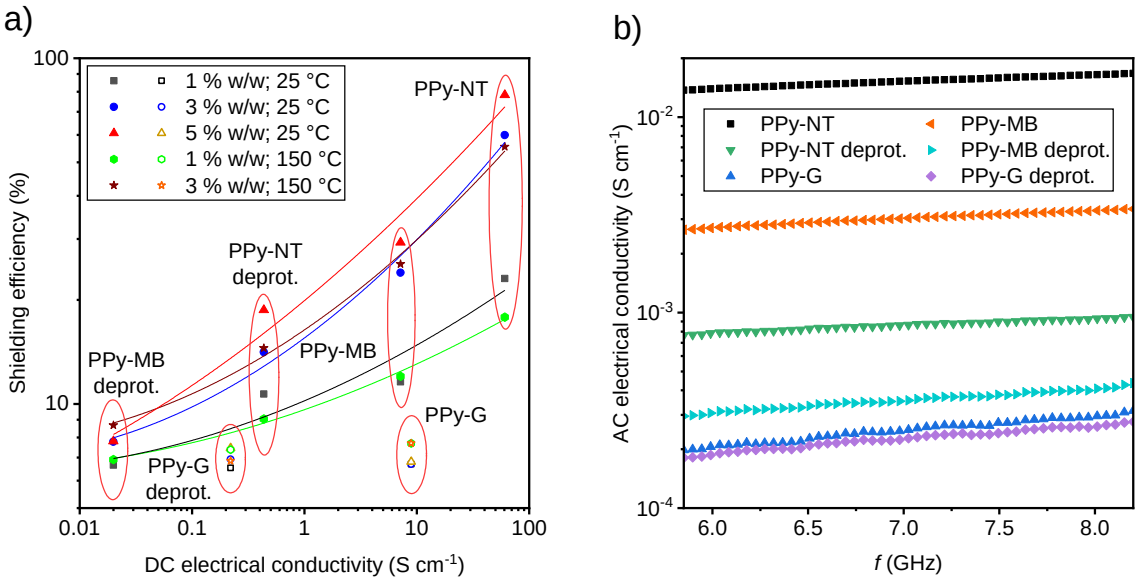

Figure 7 – a) shielding efficiency vs. electrical conductivity for various PPy morphologies at concentrations 1 and 3 % w/w and temperatures of sample preparation 25 and 150 °C; PPy-G (open symbols) not included in the trend lines, PPy-MB and PPy-NT (full symbols) included in the trend lines; samples containing 5 % w/w of PPy morphologies and cured at 150 °C are not presented due to the lower mechanical stability; b) AC electrical conductivity of PPy in silicone matrix vs. frequency (3 % w/w, 25 °C)

Several interesting observations can be made in the Figure 7. Firstly, concentration of PPy in silicone matrix plays more important role in the shielding efficiency than the second parameter – temperature of sample preparation. The difference in shielding efficiency for concentration of PPy in silicone matrix is more pronounced for samples with high electrical conductivities (over 1 S cm^{-1}). Secondly, PPy-NT exhibits the highest electrical conductivity from all samples and its deprotonated form is still

significantly more conductive than all remaining deprotonated samples. Hence, the resulting high shielding efficiency in case of PPy-NT is not so surprising and unfortunately it is difficult to clearly separate contribution of electrical conductivity and morphology to the shielding efficiency in this case. However, some minor conclusions can be made in the case of PPy-G and PPy-MB. The PPy-G and PPy-MB exhibit very similar electrical conductivities (7.2 and 8.9 S cm^{-1}, respectively) in their initial forms and higher difference in their deprotonated forms (0.2 and 2.0×10^{-2} S cm^{-1}, respectively; *i.e.* one order of magnitude difference). Nevertheless, the shielding efficiency of both initial and deprotonated PPy-G samples is always lower compared to respective PPy-MB samples, therefore this discrepancy could be assigned to the influence of PPy morphology. Low aspect ratio of PPy-G compared to PPy-MB and PPy-NT causes that its silicone composite is unable to form conducting network of similar quality at the same concentration (Figure 7b). Hence PPy-G is far from the DC conductivity trend line in the Figure 7a.

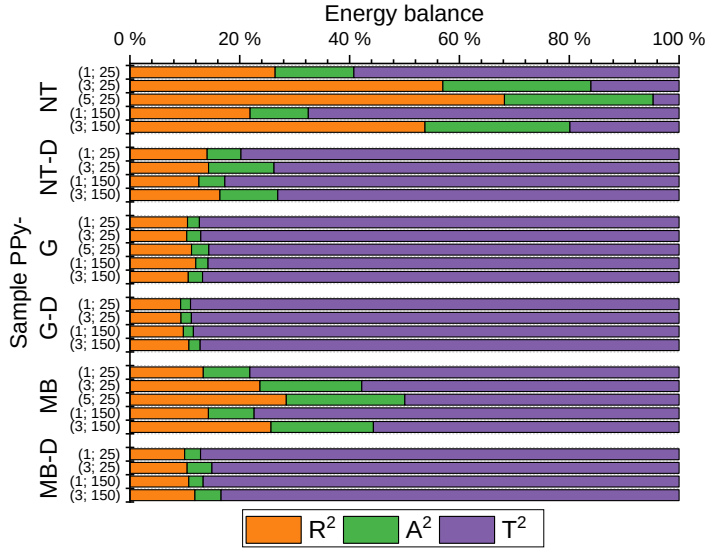

Figure 8 – The RAT (Reflection, Absorption, Transmission) analysis of all PPy samples. Y-axis gives information about concentration (1, 3, 5 % w/w) of PPy in silicone matrix and curing temperature (25 or 150 °C) of sample preparation

Figure 8 provides another view of the shielding efficiency of PPy morphologies. The relationship between reflected (*R*), absorbed (*A*), and transmitted (*T*) portions of electromagnetic wave intensity follows:

$$R^2 + A^2 + T^2 = 1 \quad (4)$$

Using this equation, direct determination of *R* and *T* from measured values of S_{11} and S_{21}, respectively, enables one to extract absorbed part (*A*) of electromagnetic wave intensity. Visualizing the proportion between the three components in "RAT analysis" (analysis of reflection, absorption, and transmission capability of each sample) clearly indicates higher absorption percentage of samples with nano- or

micro- structure, *i.e.* PPy-NT and PPy-MB, compared to the PPy-G regardless of protonation state. The high absorption ability of structured PPy is very important from the application point of view as the reflection of electromagnetic radiation from highly conductive shields usually leads to the unwanted secondary emission of EMI.

4. Conclusion

Two important conclusions can be drawn from the above results. Firstly, the shielding efficiency of uniform PPy structures in the C-band region depends namely on the absolute size of its electrical conductivity. The PPy nanotubes with electrical conductivity of 60 S cm^{-1} dispersed in the silicone matrix at relatively low concentration of 5 % w/w can shield off around 80 % of incident radiation. For the future application of PPy in EMI shielding it is therefore essential to develop nanotubes (or high aspect ratio morphology) with electrical conductivity as high as possible. So far, the highest recorded electrical conductivity of PPy-NT was 119 S cm^{-1}, which creates even more space for improvement of shielding efficiency. [22] Understandably, long term stability of such high electrical conductivity presents a challenge for EMI application. Secondly, uniform morphology of PPy increases the ability of material to absorb incident radiation and thus lowering emission of secondary EMI by reflection. This is a very important observation as many novel morphologies are currently being developed. [2] Furthermore, improvement of absorption at the expense of reflection is essential for the future EMI shields and it can be crucial for leaving commonly used reflective metallic shields.

There are two other minor conclusions regarding the sample preparation. The PPy-NT were able to shield EMI at relatively low concentration in silicone matrix. The shielding efficiency of PPy-NT in silicone matrix at 3 % w/w was S_{21} = –7.95 dB (40.1 % of transparency) whereas at 5 % w/w it was even higher S_{21} = –13.27 dB (21.7 % of transparency) but at the cost of lower mechanical stability of the sample. Therefore, future designs of EMI shields based on PPy have to also consider the use of matrixes able to contain higher concentration of PPy or improvement in compatibility between PPy and matrix. The last observation is related to the temperature of sample preparation. It was shown that preparation of the sample at 150 °C has only a minor effect on the overall shielding efficiency. This result is rather surprising as the stability of electrical conductivity of PPy at higher temperatures is generally lower. Many potential matrixes have glass transition temperature at high temperatures and hence this observation expands the range of possible matrixes.

The PPy is currently undergoing substantial transition from one of many conducting polymers belonging to the Nobel Prize awarded class of materials into the class of progressive nanomaterials whose applications are not determined only by its electrical conductivity. The morphology of PPy will play a substantial role in its future application. [23] The EMI shielding is one such application, *i.e.* it combines the best from both the electrical conductivity and morphology.

5. Acknowledgement.

This work was supported by the Ministry of Education, Youth and Sports of the Czech Republic – project DKRVO (RP/CPS/2020/006) and Specific university research – grant No A2_FCHI_2020_030.

6. References

[1] T.V. Vernitskaya, O.N. Efimov, Polypyrrole: A conducting polymer (synthesis, properties, and applications), Usp Khim+, 66 (1997) 489-505

[2] J. Stejskal, J. Prokeš, Conductivity and morphology of polyaniline and polypyrrole prepared in the presence of organic dyes, Synthetic Met, 264 (2020), ARTN 116373, DOI: 10.1016/j.synthmet.2020.116373

[3] J. Stejskal, M. Trchová, Conducting polypyrrole nanotubes: a review, Chem Pap, 72 (2018) 1563-1595, DOI: 10.1007/s11696-018-0394-x

[4] J. Stejskal, Interaction of conducting polymers, polyaniline and polypyrrole, with organic dyes: polymer morphology control, dye adsorption and photocatalytic decomposition, Chem Pap, 74 (2020) 1-54, DOI: 10.1007/s11696-019-00982-9

[5] Y.Z. Long, M.M. Li, C.Z. Gu, M.X. Wan, J.L. Duvail, Z.W. Liu, Z.Y. Fan, Recent advances in synthesis, physical properties and applications of conducting polymer nanotubes and nanofibers, Prog Polym Sci, 36 (2011) 1415-1442, DOI: 10.1016/j.progpolymsci.2011.04.001

[6] D. Kopecký, M. Varga, J. Prokeš, M. Vrňata, M. Trchová, J. Kopecká, M. Václavík, Optimization routes for high electrical conductivity of polypyrrole nanotubes prepared in presence of methyl orange, Synthetic Met, 230 (2017) 89-96, DOI: 10.1016/j.synthmet.2017.06.004

[7] S. Valtera, J. Prokeš, J. Kopecká, M. Vrňata, M. Trchová, M. Varga, J. Stejskal, D. Kopecký, Dye-stimulated control of conducting polypyrrole morphology, Rsc Adv, 7 (2017) 51495-51505, DOI: 10.1039/c7ra10027b

[8] J. Stejskal, M. Trchová, P. Bober, Z. Moravková, D. Kopecký, M. Vrňata, J. Prokeš, M. Varga, E. Watzlová, Polypyrrole salts and bases: superior conductivity of nanotubes and their stability towards the loss of conductivity by deprotonation, Rsc Adv, 6 (2016) 88382-88391, DOI: 10.1039/c6ra19461c

[9] J. Prokeš, M. Varga, M. Vrňata, S. Valtera, J. Stejskal, D. Kopecký, Nanotubular polypyrrole: Reversibility of protonation/deprotonation cycles and long-term stability, Eur Polym J, 115 (2019) 290-297, DOI: 10.1016/j.eurpolymj.2019.03.037

[10] M. Varga, D. Kopecký, J. Kopecká, I. Křivka, J. Hanuš, A. Zhigunov, M. Trchová, M. Vrňata, J. Prokeš, The ageing of polypyrrole nanotubes synthesized with methyl orange, Eur Polym J, 96 (2017) 176-189, DOI: 10.1016/j.eurpolymj.2017.08.052

[11] D.W. Jiang, V. Murugadoss, Y. Wang, J. Lin, T. Ding, Z.C. Wang, Q. Shao, C. Wang, H. Liu, N. Lu, R.B. Wei, A. Subramania, Z.H. Guo, Electromagnetic Interference Shielding Polymers and Nanocomposites-A Review, Polym Rev, 59 (2019) 280-337, DOI: 10.1080/15583724.2018.1546737

[12] P. Kumar, U.N. Maiti, A. Sikdar, T.K. Das, A. Kumar, V. Sudarsan, Recent Advances in Polymer and Polymer Composites for Electromagnetic Interference Shielding: Review and Future Prospects, Polym Rev, 59 (2019) 687-738, DOI: 10.1080/15583724.2019.1625058

[13] A.M. Xie, F. Wu, M.X. Sun, X.Q. Dai, Z.H. Xu, Y.Y. Qiu, Y. Wang, M.Y. Wang, Self-assembled ultralight three-dimensional polypyrrole aerogel for effective electromagnetic absorption, Appl Phys Lett, 106 (2015), Artn 222902, DOI: 10.1063/1.4921180

[14] A.M. Xie, K. Zhang, M.X. Sun, Y.L. Xia, F. Wu, Facile growth of coaxial Ag@polypyrrole nanowires for highly tunable electromagnetic waves absorption, Mater Design, 154 (2018) 192-202, DOI: 10.1016/j.matdes.2018.05.039

[15] Y.Z. Jiao, J.J. Li, A.M. Xie, F. Wu, K. Zhang, W. Dong, X.F. Zhu, Confined polymerization strategy to construct polypyrrole/zeolitic imidazolate frameworks (PPy/ZIFs) nanocomposites for tunable electrical conductivity and excellent electromagnetic absorption, Compos Sci Technol, 174 (2019) 232-240, DOI: 10.1016/j.compscitech.2019.03.003

[16] A.M. Xie, F. Wu, W.C. Jiang, K. Zhang, M.X. Sun, M.Y. Wang, Chiral induced synthesis of helical polypyrrole (PPy) nano-structures: a lightweight and high-performance material against electromagnetic pollution, J Mater Chem C, 5 (2017) 2175-2181, DOI: 10.1039/c6tc05057c

[17] V. Babayan, N.E. Kazantseva, R. Moučka, J. Stejskal, Electromagnetic shielding of polypyrrole-sawdust composites: polypyrrole globules and nanotubes, Cellulose, 24 (2017) 3445-3451, DOI: 10.1007/s10570-017-1357-z

[18] S.C. Hu, Y. Zhou, L.L. Zhang, S.J. Liu, K. Cui, Y.Y. Lu, K.N. Li, X.D. Li, Effects of indigo carmine concentration on the morphology and microwave absorbing behavior of PPy prepared by template synthesis, J Mater Sci, 53 (2018) 3016-3026, DOI: 10.1007/s10853-017-1702-5

[19] A.M. Nicolson, G.F. Ross, Measurement of Intrinsic Properties of Materials by Time-Domain Techniques, Ieee T Instrum Meas, Im19 (1970) 377-382, DOI: 10.1109/Tim.1970.4313932

[20] W.B. Weir, Automatic Measurement of Complex Dielectric-Constant and Permeability at Microwave-Frequencies, P Ieee, 62 (1974) 33-36, DOI: 10.1109/Proc.1974.9382

[21] M. Green, T. Anh Thi Van, C. Xiaobo, Maximizing the Microwave Absorption Performance of Polypyrrole by Data-Driven Discovery, Compos Sci Technol, 199 (2020) 108332, DOI: 10.1016/j.compscitech.2020.108332

[22] Y. Li, P. Bober, M. Trchova, J. Stejskal, Polypyrrole prepared in the presence of methyl orange and ethyl orange: nanotubes versus globules in conductivity enhancement, J Mater Chem C, 5 (2017) 4236-4245, DOI: 10.1039/c7tc00206h

[23] J. Stejskal, Conducting polymers are not just conducting: A perspective for emerging technology, Polymer International, (2019), DOI: 10.1002/pi.5947